HYDRODYNAMIC CHARACTERISTICS OF POLYGONAL CONTOURS IN SUPERCAVITATING FLOW

Y. N. Savchenko, V. N. Semenenko, and Y. I. Naumova
Ukraine National Academy of Sciences
Institute of Hydromechanics
Kiev, Ukraine

A. N. Yarghese, J. S. Uhlman, and I. N. Kirschner
Naval Undersea Warfare Center Division
Newport, Rhode Island 02841-1708 U. S. A.

ABSTRACT

The nature of the hydrodynamic forces on an axisymmetric cavitator with a polygonal generatrix is investigated using analytical and numerical methods. The changes in the forces and moment with changes in yaw angle are considered for various cavitator shapes. The exact solution of the analogous two-dimensional problem is first determined using free-streamline theory and conformal mapping, and extended to estimate the forces on axisymmetric cavitators. The results of a fully-axisymmetric boundary-element computation are then compared with the analytical results. The conditions of static stability of the polygonal cavitator are obtained. The possibility is discussed of controlling the cavity dimensions by altering the cavitator shape and thus modifying the associated drag coefficient.

INTRODUCTION

The cavitation number, σ, is an important parameter of supercavitating flows:

$$\sigma \triangleq \frac{2(pgh - p_c)}{\rho V_\infty^2}, \tag{1}$$

where h and V are the depth and the speed of motion, respectively, and p_c is the cavity pressure. The midsection diameter, D_c, and the length, L_c, of a stationary axisymmetric supercavity do not depend on the cavitator shape for small σ. They are determined by its diameter, D_n, the drag coefficient, c_x, and the cavitation number (Garabedian, 1956):

$$D_c = D_n\sqrt{\frac{c_x}{\sigma}}, \quad L_c = \frac{D_n}{\sigma}\sqrt{c_x \ln\frac{1}{\sigma}}. \tag{2}$$

The following approximate formula for the drag coefficient of a blunted cavitator is valid at small cavitation numbers (Logvinovich, 1969):

$$c_x \triangleq c_{x0}(1+\sigma), \tag{3}$$

where c_{x0} is the drag coefficient value for a given cavitator when $\sigma = 0$ (that is, for free streamline flow).

The validity of these asymptotic formulae has been confirmed experimentally for models with disk cavitators moving with speeds ranging from 300 to 1200 m/s (Savchenko, et al, 1992).

The shape of nonaxisymmetric cavitators becomes important for solving dynamic problems concerning the stability of rectilinear motion and for computing the trajectory of supercavitating bodies. Account of the cavitator shape is especially important for high speeds of motion, say V~1000 m/s. In such cases, even small discrepancies of workmanship can result in appreciable cross force because of the high velocity head, $\rho V^2/2$. Nonaxisymmetric cavitators are also applied in practice, for example, to create the lift compensating for gravity for horizontal underwater motion at moderate speeds (Logvinovich, 1969; Tzeitlin, et al, 1993).

Effective methods of numerical prediction of axisymmetric cavity flows based on the exact problem statement have been validated for moderate values of the cavitation number (Brennen, 1969; Guzevsky, 1979; Ivanov, 1980; Deynekin, 1994). In particular, a desktop computer program has been developed at the IHM UNAS (Ivanov, 1980). It allows computation of cavities behind axisymmetric cavitators of practical arbitrary shape, including those with a concave face directed upstream and cavitators with an inlet. However, similar computational methods for nonaxisymmetric cavitators or nonzero yaw angles are not known to these authors.

The dependence of the hydrodynamic forces on the yaw angle are determined experimentally in practice. However, the nature of such dependence can be evaluated using the solution for the two-dimensional problem of free-streamline flow around a contour representing a meridional section of the cavitator-cavity system. Assume that the generatrix of the cavitator represents a four-sided polygon, $ABCDE$, symmetric relative to the axis passing through the vertex as shown in figure 1a. Also, assume that the cavity detaches at the fixed, salient points, A and E. Note that this method is easily applied to polygonal contours with more than four segments.

The exact solution of the two dimensional problem may be used for the estimation of drag in cases of flow around axisymmetric cavitators at zero yaw angle. The pressure distribution, p, along the generatrix of the cavitator is taken from the solution of the two dimensional problem of free-streamline flow around the contour coinciding with a meridional section of the cavitator. Then the drag is approximated by integration:

$$\tilde{c}_x \triangleq \frac{\tilde{X}}{\frac{\pi}{2}\rho V_\infty^2 R_n^2}, \quad \tilde{X} \triangleq 2\pi \int_0^{R_n} (p - p_c) y dy , \tag{4}$$

where $R_n = D_n/2$. This approach is not rigorous; however, for disks and cones this method predicts drag values close to experimental data (Plesset, et al, 1948; Birkgof, et al, 1957).

FREE-STREAMLINE FLOW PAST POLYGONAL CONTOURS

The scheme of free-streamline flow past the four-sided, symmetric, two-dimensional, polygonal contour $ABCDE$ with the axis inclined at an angle α to the free stream is adduced in figure 1. The lengths of internal segments BC and CD are both equal to b and they make an angle $\pi\mu$ with the x-axis. The lengths of the external segments are equal to a and they make an angle $\pi\gamma$ with the x-axis.

The solution of the problem is constructed by Chapligin's method of singular points (Gurevich, 1979; Fedorov, 1960) by means of a conformal transformation of the physical flow of complex potential W onto the first quadrant of the plane of the parametric complex variable $u = \xi + i\eta$

$$\frac{dW}{du} = 4\varphi_0(1+\varepsilon^2)\frac{(1+u^2)u}{(\varepsilon^2+u^2)^3}, \tag{5}$$

$$\frac{dW}{dz} = V_\infty e^{i\pi\gamma}\frac{u-i}{u+i}\left(\frac{u-i\nu}{u+i\nu}\right)^{2\mu-1}\left(\frac{u-i\lambda}{u+i\lambda}\right)^{\gamma-\mu}\left(\frac{u-i\kappa}{u+i\kappa}\right)^{\gamma-\mu}. \tag{6}$$

Here $dW/dz = V\exp(-i\theta)$ is the complex velocity and φ_0 is the value of potential at the cavity detachment point, A. Using the condition on the free streamlines $V=V_\infty$ from equation 6, it is easy to obtain the expression for the slope of the free streamlines:

$$\theta(\xi) = \pi\gamma + 2\arctan\frac{1}{\xi} + 2(2\mu-1)\arctan\frac{\nu}{\xi} + 2(\gamma-\mu)\left(\arctan\frac{\lambda}{\xi} + \arctan\frac{\kappa}{\xi}\right). \tag{7}$$

A conformity of points of the physical and the parametric complex planes is expressed in the form:

$$z(u) = \int_i^u \frac{dz}{dW}\frac{dW}{du}du. \tag{8}$$

Solution 5-6 contains five real parameters: $\varphi_0 > 0$, $0 < \varepsilon < \infty$, and $0 \le \lambda < \nu \le 1 < \kappa < \infty$. The kinematic condition at infinity, $\theta(\varepsilon) = \alpha$, and four conditions defining the lengths of the segments are then applied:

$$\int_0^\lambda \Phi(\eta)d\eta = a, \quad \int_\lambda^\nu \Phi(\eta)d\eta = 1,$$
$$\int_\nu^\kappa \Phi(\eta)d\eta = 1, \quad \int_\kappa^\infty \Phi(\eta)d\eta = a, \tag{9}$$

where all lengths have been scaled with b, and where :

$$\Phi(\eta) \triangleq \frac{4\varphi_0(1+\varepsilon^2)}{V_\infty}\left|\frac{\eta+\nu}{\eta-\nu}\right|^{2\mu-1} \times \left|\frac{(\eta+\lambda)}{(\eta-\lambda)}\frac{(\eta+\kappa)}{(\eta-\kappa)}\right|^{\gamma-\mu}\frac{(1+\eta)^2\eta}{(\varepsilon^2+\eta^2)^3}. \tag{10}$$

Except for two unknowns, it is possible to obtain a system of three functional equations for three unknowns, which may be solved numerically by Newton's method (Romanovsky, et al, 1970). The quadratures are computed by Gauss' method, accounting for the singularities of the integrands. After defining the transformation parameters and the scale factor, φ_0/bV_∞, all the flow characteristics can be computed. The pressure distribution along the contour is:

$$C_p = \frac{p-p_\infty}{\frac{1}{2}\rho V_\infty^2} = 1 - \left(\frac{V}{V_\infty}\right)^2 = 1 - \left(\frac{\eta-1}{\eta+1}\right)^2\left(\frac{\eta-\nu}{\eta+\nu}\right)^{2(2\mu-1)}\left(\frac{\eta-\lambda}{\eta+\lambda}\right)^{2(\gamma-\mu)}\left(\frac{\eta-\kappa}{\eta+\kappa}\right)^{2(\gamma-\mu)} \tag{11}$$

The complex force acting on the contour (Gurevich, 1979) is

$$X + iY = \pi\rho V_\infty e^{-i\alpha}\mathrm{Res}\left(V_\infty\frac{dz}{dW}\frac{dW}{du}\right)_{u=\varepsilon} \tag{12}$$

from which the force and moment coefficients are computed as

$$c_x \triangleq \frac{X}{\rho V_\infty^2 R_n}$$

$$= 2\pi \frac{\varphi_0}{bV_\infty} \frac{\left(1+\varepsilon^2\right)^2}{\varepsilon^2}$$

$$\times \left\{ \frac{1}{1+\varepsilon^2} + (2\mu - 1) f_1(\nu) + (\gamma - \mu)\left[f_1(\lambda) + f_1(\kappa) \right] \right\}^2 ,$$

$$c_y \triangleq \frac{Y}{\rho V_\infty^2 R_n} \qquad (13)$$

$$= \pi \frac{\varphi_0}{bV_\infty} \frac{1+\varepsilon^2}{\varepsilon^3}$$

$$\times \left\{ \frac{\varepsilon^2 - 1}{\varepsilon^2 + 1} + (2\mu - 1) f_2(\nu) + (\gamma - \mu)\left[f_2(\lambda) + f_2(\kappa) \right] \right\} ,$$

$$c_m \triangleq \frac{M_0}{2\rho V_\infty^2 R_n^2} ,$$

where the moment is that about the contour center:

$$M_0 = \mathrm{Re}\left\{ \int_A^E (p - p_\infty) z d\bar{z} \right\}$$

$$= \frac{\rho V_\infty^2}{2} \int_0^\infty C_p(\eta) \left[x(\eta) \frac{dx}{d\eta} + y(\eta) \frac{dy}{d\eta} \right] d\eta .$$

The other quantities appearing in these expressions are:

$$R_n \triangleq \sin(\pi\mu) + a \sin(\pi\gamma)$$

and:

$$f_1(s) \triangleq \frac{s}{\varepsilon^2 + s^2}, \quad f_2(s) \triangleq \frac{s\left[\varepsilon^2\left(\varepsilon^2 - 3\right) + s^2\left(3\varepsilon^2 - 1\right)\right]}{\left(\varepsilon^2 + s^2\right)^2}.$$

The coordinates of contour points $x(\eta)$ and $y(\eta)$ are computed using equation 8 with $\zeta = 0$. The coordinates of points on the upper $(0 < \xi < \varepsilon)$ and lower $(\varepsilon < \xi < \infty)$ free streamlines are computed using equation 8 with $\eta = 0$.

THE INFLUENCE OF VISCOUS DRAG

This method for predicting the hydrodynamic characteristics of free-streamline flow around polygonal contours was applied to sharp wedges at small yaw angles for prediction of flows past underwater foils and struts (Fedorov, 1960; Romanovsky, et al, 1970; et cetera). In such cases, the lift computation has practical significance. The predicted dependence of drag on yaw angle does not correspond to experimental data, because viscous drag (which is dominant for sharp wedges) has been neglected. On the other hand, cavity drag dominates in the case of a blunt cavitator at small values of the cavitation number.

THE PHYSICAL REALIZABILITY OF TWO-DIMENSIONAL SUPERCAVITATING FLOWS

We chose the generalized polygonal approximation of the cavitator contour with the purpose of development of a fast algorithm on a desktop computer. It is known that the flow speed is infinite at an exterior angle (Gurevich, 1979). Accordingly, the pressure is negatively infinite. Experience shows that this local rarefaction frequently has a poor influence on the global hydrodynamic behavior of the contour. Local separation or cavitation may occur in practice near the angular points of the contour.

Inflection points on a free streamline can also occur in certain cases owing to the presence of angular points on the contour. For example, it occurs for wedges when the yaw angle, α, exceeds some critical value α_{cr}. The position of the inflection point on the free streamline is defined from the condition $\theta'(\xi) = 0$, from which:

$$\frac{1}{1+\xi^2} + \frac{\nu(2\mu - 1)}{\nu^2 + \xi^2} + \frac{(\gamma - \mu)(\lambda + \kappa)\left(\lambda\kappa + \xi^2\right)}{\left(\lambda^2 + \xi^2\right)\left(\kappa^2 + \xi^2\right)} = 0 . \qquad (14)$$

Equation 14 is easily reduced to a cubic equation in ξ^2.

Thus, two additional constraints limit the selection of the contour segment angles γ and μ for physically-realizable free-streamline flow with cavity detachment at points A and E. Firstly, for $\gamma = 0$, the free streamlines must be strictly convex according to Brillouin's principle (Birkgof and Sarantonello, 1957; Romanovsky, et al, 1970). Secondly, γ must be greater than μ, since otherwise the cavity would detach at D or B (depending on the yaw angle, α), rather than at A and E, due to the summary rarefaction in the neighborhood of the exterior angle.

The condition of the existence of an inflection point follows from equation 14 in the specific case of a wedge, $\gamma = \mu$:

$$\frac{\nu + 2\mu - 1}{1 + \nu(2\mu - 1)} < 0 . \qquad (15)$$

For $\nu > 0$, it is obvious that an inflection point cannot exist for $\mu > 0.5$.

Equation 15 has no roots for the plate, $\gamma = \mu = 0.5$. That is, an inflection point is not present for any α. Analysis of the roots of equation 14 is executed numerically for cavitators of arbitrary shape.

The predicted flow reorganization as the yaw angle increases beyond α_{cr} for sharp wedges has been observed experimentally (Savchenko, et al, 1997): a hysteresis loop takes place in the experiments with consecutive increase and reduction of the angle α.

DRAG OF AXISYMMETRIC CAVITATORS

Practical extimation of the cavitator drag involves computing the pressure distribution, p, along the cavitator generatrix from the solution of the two-dimensional free-streamline flow. The drag of the axisymmetric cavitator is then estimated using formula 4. Plesset, et al, (1948) show that the values, c_x, for cones computed this way are close to experimental data. Comparison with numerical solutions of the exact problem is facilitated by employing the formulae proposed by Guzevsky (1983):

$$c_x = c_{x0} + (0.524 + 0.672\mu)\sigma, \quad 0 \le \sigma \le \frac{1}{4}, \quad 0 \le \mu \le \frac{1}{2}$$

$$c_{x0} = \begin{cases} \mu(0.915 + 9.5\mu), & 0 < \mu < \dfrac{1}{12} \\ 0.5 + 1.81(\mu - 0.25) - 2(\mu - 0.25)^2, & \dfrac{1}{12} < \mu < \dfrac{1}{2} \end{cases} \qquad (16)$$

where $\pi\mu$ is the semiangle of the cone. The values c_{x0} (that is, for $\sigma \to 0$) are obtained by extrapolation. A comparison of the experimental data with the results of exact (Guzevsky, 1983) and approximate (Plesset, et al, 1948) computations is adduced in table 1:

$\pi\mu$	15°	30°	45°	60°	75°	90°
Experiment	0.15	0.35	0.47	0.61	0.72	0.82
c_{x0} [1]	0.1428	0.3353	0.5000	0.6369	0.7461	0.8275
$\tilde{c}_{x0}$ [2]	0.2045	0.3758	0.5181	0.6350	0.7296	0.8053

1 (Guzevsky, 1983)
2 (Plesset, et al, 1948)

The value for an arbitrary contour is estimated from equation 4:

$$\tilde{c}_{x0} = \frac{2}{R_n^2}\int_0^1 C_p(\eta)\, y(\eta)\frac{dy}{d\eta}\, d\eta \ . \qquad (17)$$

PROGRAM FLOWJET

The desktop computer program FLOWJET has been developed at IHM UNAS to carry out the computations using formulae 7 through 16. For given values, a/b, μ, γ, and α, the program computes:

- the coefficients c_x, c_y, c_m;
- the shapes of the free streamlines;
- the coefficients of the rotational derivatives c_x^α, c_y^α, c_m^α;
- the coefficient $\tilde{c}_x$ for an axisymmetric cavitator;
- the position of the critical point, O, on the contour; and,
- the coordinates of any inflection point of the free streamlines.

The program has a convenient user interface and displays the results on the terminal in graphical form. Examples of application of the method described above using program FLOWJET are submitted below.

PROGRAM SCAX

The desktop computer program SCAX has been developed at NUWCDIVNPT to predict axisymmetric flows past supercavitating bodies (Kirschner, et al, 1995). The program computes irrotational supercavitating flows of incompressible fluids past bodies of revolution at zero angle of attack using fully-axisymmetric boundary elements. This program has been used to validate the circumferential integration for approximating drag, equations 4, and to verify some of the numerical results presented below.

The accuracy of program SCAX has been discussed in detail in Kirschner, et al, (1995). Since publication of that article, the program has been improved in various ways, notably via elimination of an error in the computation of total drag once the potential flow problem has been solved. Additional validation has been based on comparison with the Guzevsky approximation, equations 16. Figure 2 presents a comparison of the drag predicted by program SCAX with the Guzevsky drag approximation from the exact solution for axisymmetric supercavitating flow past a cone. It can be seen that the numerical results are excellent over the entire range of cone angles compared (from 10° through 90° semi-angle) for values of the cavitation number, σ, of 0.077 and 0.100. This represents a generalization of the circumferentially-integrated free-streamline approximation described above, since the results can be extended to non-zero cavitation numbers, albeit at the cost of additional computation, and with the limitation that program SCAX cannot predict non-axisymmetric flows.

Additional comparison of the free-streamline results with those of program SCAX will be presented in the discussion of some of the examples described below.

STATICALLY STABLE CONTOURS

The pressure forces acting on the inclined contours in free-streamline flow sum to the resultant force, $\bar{F}$, and moment, M_0, shown in figure 3. The contour will be statically stable if these forces tend to turn the cavitator to decrease angle α relative to the mass center of the model. The condition of static stability has the form:

$$\delta = \arctan\frac{F_y}{F_x} > \alpha \ , \qquad (18)$$

where F_x and F_y are the projections of the vector $\bar{F}$ onto the x- and y-axes.

Computations have shown that a cavitator is statically stable if its contour is concave towards the stream (in particular, inverted wedges with $\mu > 0.5$). A flat plate will be neutrally stable, $F_y/F_x = \tan\alpha$, if we do not take into account the moment M_0 induced by displacement of the point of application of force $\bar{F}$ from the point C. Computations have shown that this moment is always stabilizing, but is very small in value. Convex contours (in particular, wedges with $\mu < 0.5$) are statically unstable.

The force polars for wedges are adduced in figure 4 for a series of values of wedge semiangle, $\beta = \pi\mu$, in degrees. The characteristic stability regions are shown in figure 5. Wedges are statically stable for $\beta > 90°$ and are statically unstable for $\beta < 90°$. The lift of a wedge is equal to 0 irrespective of the yaw angle for $\beta \approx 50°35'$.

Program FLOWJET allows selection of the best cavitator shape for static stability for which the arbitrary c_y^α is maximum. The best cavitator from a practical point of view: (1) is statically stable; (2) has a maximal rotational derivative c_y^α; and, (3) has a minimal drag coefficient c_{x0}. The following question is interesting: Do statically stable contours exist which have lower drag than the flat plate? Computations have shown that for such contours $\mu > 0.5$, $\gamma < 0.5$, and $a/b \sim 0.1$. Theoretically physically realizable members of this set exist, as defined above. However, the final answer to this question requires additional experimentation.

CONTROL OF CAVITY DIMENSIONS

It is apparent from equation 2 that control of supercavity dimensions for constant D_n, h, and V_∞ is possible by two techniques: (1) changing the cavitation number, σ; and, (2) changing the cavity drag coefficient, c_x. The first technique is used for speeds of motion ranging from 10 to 100 m/s and is realized by gas-supply to the cavity, that is, by increase of p_c. This approach is impractical for very large speeds of motion or small dimensions of the body. Therefore, the possibility of supercavity control by changing c_x is very interesting.

Both the length and the maximum diameter of the cavity are proportional to $\sqrt{c_{x0}}$ as is visible from equations 2 and 3:

$$\frac{D_c}{D_n} = \sqrt{\frac{c_{x0}(1+\sigma)}{\sigma}}, \quad \frac{L_c}{D_n} = \frac{1}{\sigma}\sqrt{c_{x0}(1+\sigma)\ln\frac{1}{\sigma}} .$$

Hence the supercavity shape should change self-similarly by variation of the parameter c_{x0} at constant D_n and σ. This can be realized by changing the cavitator shape while maintaining a constant diameter of the salient edge.

Such an axisymmetric cavitator with variable geometry is proposed in figure 6. The meridional section of the cavitator has the Σ-shaped contour $\mu < 0.5$, $\gamma = 1$. The cavity drag coefficient is increased from $c_x(\mu)$ up to 1 by moving the internal cone relative to the outside cartridge, that is, by increasing parameter a from 0. This dependence of c_{x0} on a/b is shown in figure 6 for Σ-shaped contours. The dependence of the ratio $\tilde{c}_{x0}$ for axisymmetric cavitators to the value computed using free-streamline theory with the circumferential integration approximation of the drag coefficient for a disk, 0.82, on the dimensionless extension of the cavitating edge, x/D_n, is shown in figure 7a, along with experimental data. Results of Program SCAX are plotted in figure 7b. It can be seen that the results of the analytical approximation based on circumferential integration of the free-streamline results agree quite well with those of the numerical computation using the fully-axisymmetric boundary element method, but that both methods overpredict the empirical results.

This slower increase of the the experimental values of drag with an increase of x (as compared with the analytical and numerical results) is due to the zones of vortical motion formed in the interior angles of the cavitator in the experiment. In other words, potential, free-streamline flow with a critical point is not realized in the experiment; rather flow with stagnant zones is realized (Gurevich, 1979).

Photographs of supercavities for two extreme positions of the cartridge ($\sigma = 0.077$, $\mu = 1/3$) are adduced in figure 8. By extending the cavitating edge from $x/D_n = 0$ to $x/D_n = 0.138$ in the experiment, the major dimensions of the supercavity increased 35%. Figure 8 also presents predictions of the cavity shapes for two different positions of the cartridge ($\sigma = 0.17$, $\mu = {}^1/_3$) using program SCAX. It can be seen that the basic effect observed in the experiments is reflected in the numerical results. Note that the wall-shaped cavity termination is associated with the modified Riabouchinsky approximation implemented in program SCAX. A more exact comparison of the numerical and experimental results must await refinement of the program to allow prediction of flows at lower cavitation numbers: the current algorithm is limited by an ill-conditioned matrix at very large cavity lengths.

Computations using the circumferentially-integrated free-streamline technique show that the Σ-shaped contours are always statically stable for $a \neq 0$.

ACKNOWLEDGEMENTS

Research, development, and testing performed under the Naval Undersea Warfare Center Division, Newport (NUWCDIVNPT) Supercavitating High Speed Bodies (SHSB) program, C. Curtis, program manager, I. Kirschner, chief engineer. Initial feasibility testing, assessment, and range development supported by the NUWCDIVNPT Bid and Proposal (B&P) program (Fiscal Year 1996 Job Order #796C02 and #796F04). Research sponsored by the Office of Naval Research (ONR) Undersea Weaponry Basic Research program, J. Fein, program manager (Program Element 0601153N, R&D Project #BR02301) and the NUWCDIVNPT Independent Research (IR) program, S. Dickinson, program manager (Program Element 0601152N, R&D Project #RR00N04). Development sponsored by the (ONR) Undersea Weaponry Exploratory Development program, S. Beermann, program manager (Program Element 0602633N, R&D Project #01434). Feasibility testing sponsored by the Advanced Research Projects Agency (ARPA), T. Kooij, program manager (Program Element 0603569E).

REFERENCES

Birkgof, G., and E. Sarantonello (1957), *Jets, Wakes, and Cavities*, Academic Press, New York.

Brennen, C.A. (1969), "Numerical Solution for Axisymmetric Cavity Flows," *J. Fluid Mech.*, 37.

Deynekin, Y.P. (1994), "Caviting Flow Around Bodies with an Inlet," *Hydromechanics.* (In Russian.)

Fedorov, Y.A. (1960), "Motion of Wedge with Cheekbones Under Free Surface in Ideal Weightless Fluid," *Tr. TzAGI.* (In Russian.)

Garabedian, P.R. (1956), "Calculation of Axially Symmetric Cavities and Jets," *Pac. J. Math.*

Gurevich, M.I. (1979), *Theory of Jets in Ideal Fluid*, 2nd edition, M. Nauka. (In Russian.)

Guzevsky, A.G. (1979), "Numerical Analysis of Cavitating Flows," SDAS TR, Institute of Thermal Physics, SD of AS of USSR, preprinted in *Novosibrisk.* (In Russian.)

Guzevsky, A.G. (1983), "Approximating Dependence of Axisymmetric Cavities Behind Cones: Hydrodynamic Flows and Wave Processes," *Novosibirsk*, Inst. of Thermal Physics of SD of AS of USSR (In Russian.)

Ivanov, A.N. (1980), "Hydrodynamics of Supercavitating Flows," *L. Sudostroenie.*

Kirschner, I.N., J.S. Uhlman, A.N. Varghese, and I.M. Kuria (1995), "Supercavitating Projectiles in Axisymmetric Subsonic Liquid Flows," FED 210 *Cavitation and Multiphase Flow*, American Society of Mechanical Engineers, New York.

Logvinovich, G.V. (1969), *Hydrodynamics of Flows with Free Boundaries*, Naukova Dumka, Kiev. (In Russian.)

Plesset, M.S., and P.A. Shaffer (1948), "Cavity Drag in Two and Three Dimensions," *J. Appl. Phys.* 19.

Romanovsky, B.I., Y.A. Fedorov, and Z.I. Kramina (1970), "Calculation of Hydrodynamic Characteristics of Wedges in a Boundless, Weightless Fluid," *Tr. TzAGI.* (In Russian.)

Savchenko, Y.N., V.N. Semenenko, and Y.I. Naumova (1997), statement of experimental observations in initial manuscript of this article.

Savchenko, Y.N., V.N. Semenenko, and V.V. Serebryakov (1992), "Experimental Research into Supercavitating Flows at Subsonic Speeds," *Doklady AN Ukranini.* (In Russian.)

Tzeitlin, M.Y., and V.M. Lapin (1993), "Free-Streamline Flow Around Polygonal Contours with Channel Supplied Fold to Generate Lift," *Tr. TzAGI.* (In Russian.)

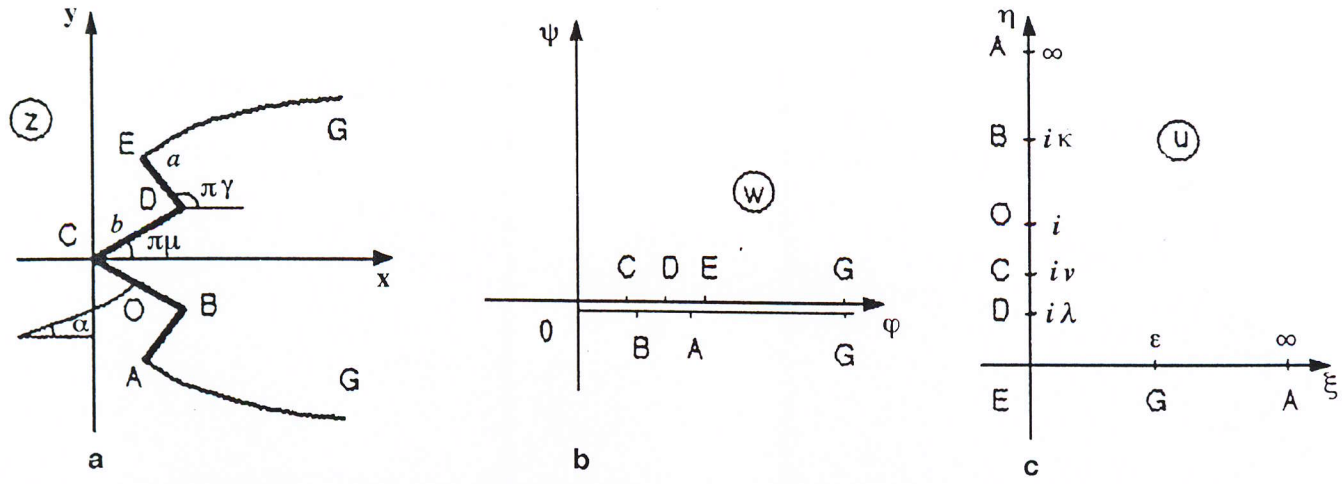

Figure 1. The Problem of Free-Streamline Flow Past an Inclined Polygonal Contour

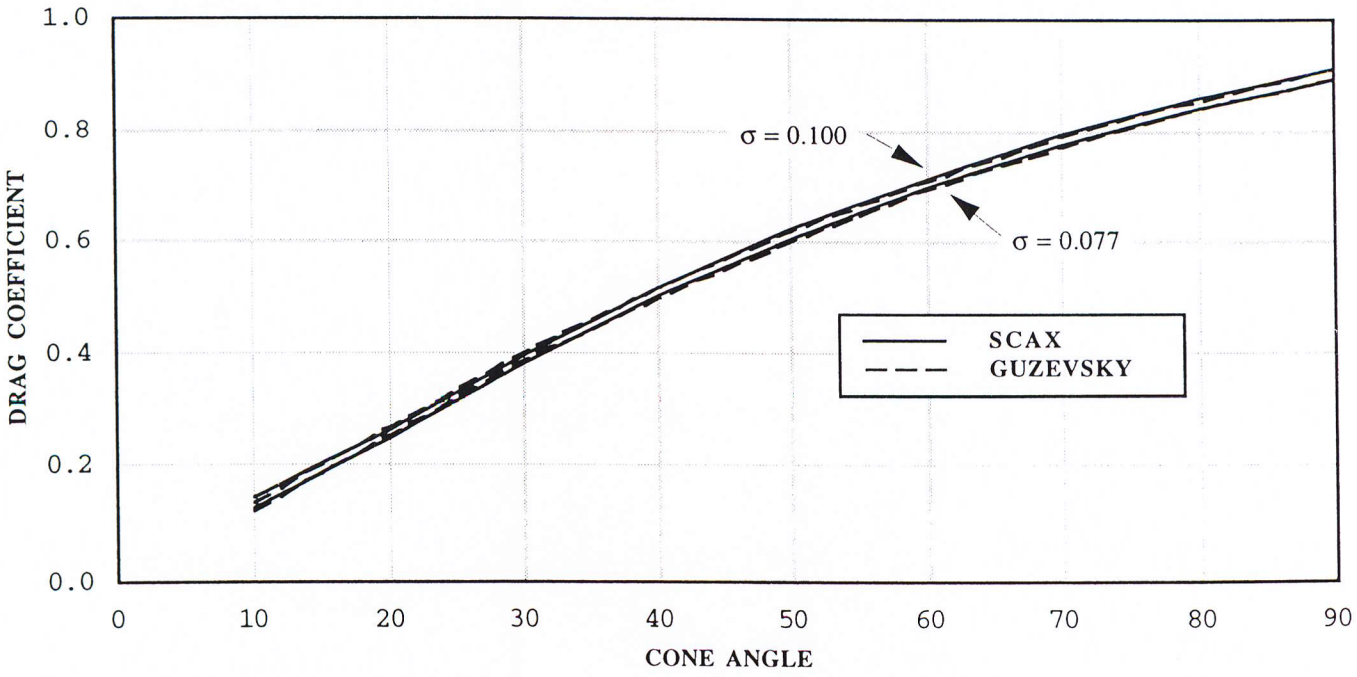

Figure 2. Comparison of Drag Computed Using a Fully-Axisymmetric Boundary-Element Method (Program SCAX) with Guzevsky's Approximation to the Exact Solution for Supercavitating Flow Past a Cone

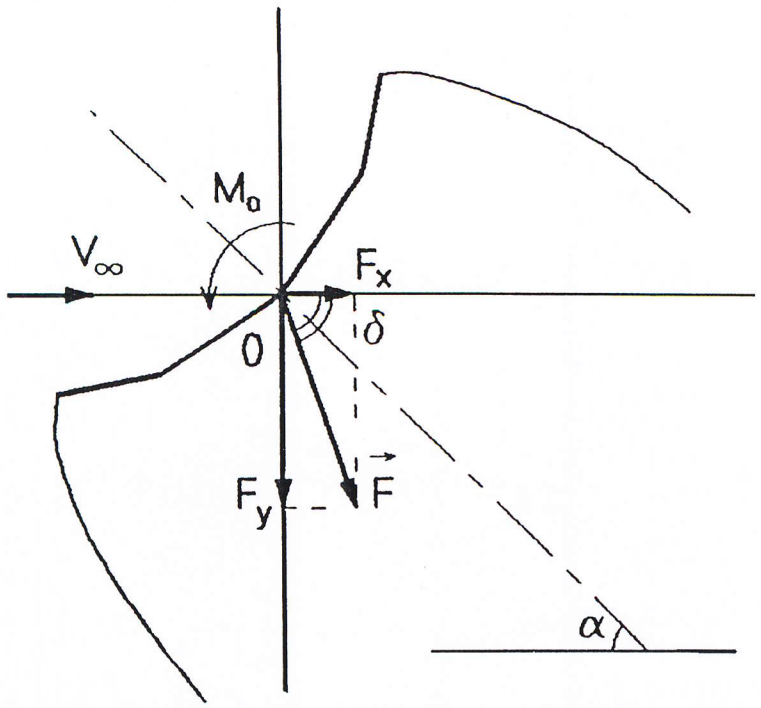

Figure 3. Forces Acting on an Inclined Polygonal Contour

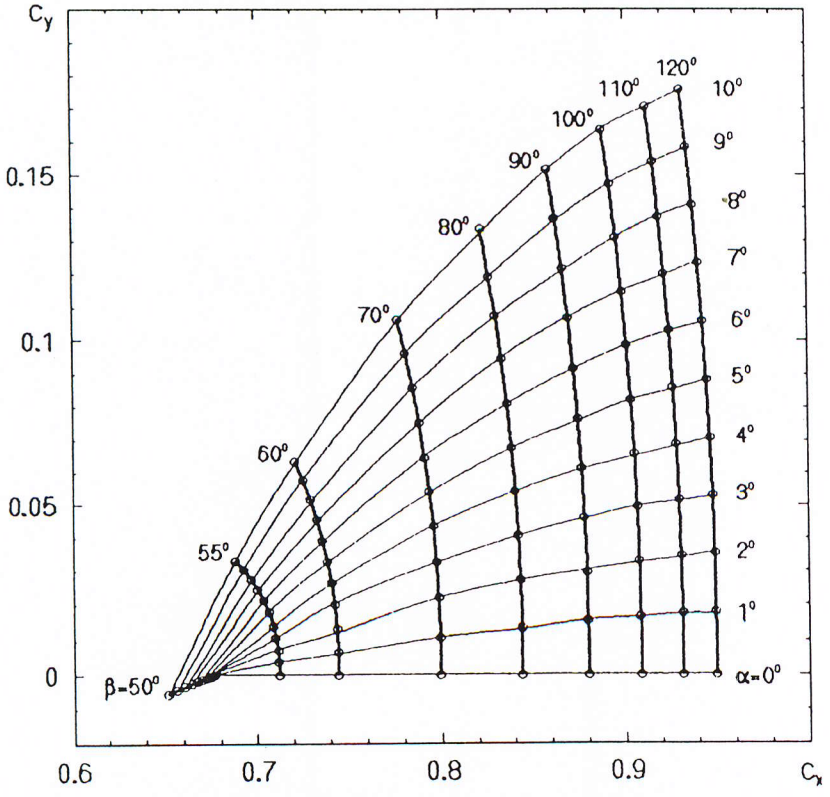

Figure 4. Force Polars for Wedge Cavitators

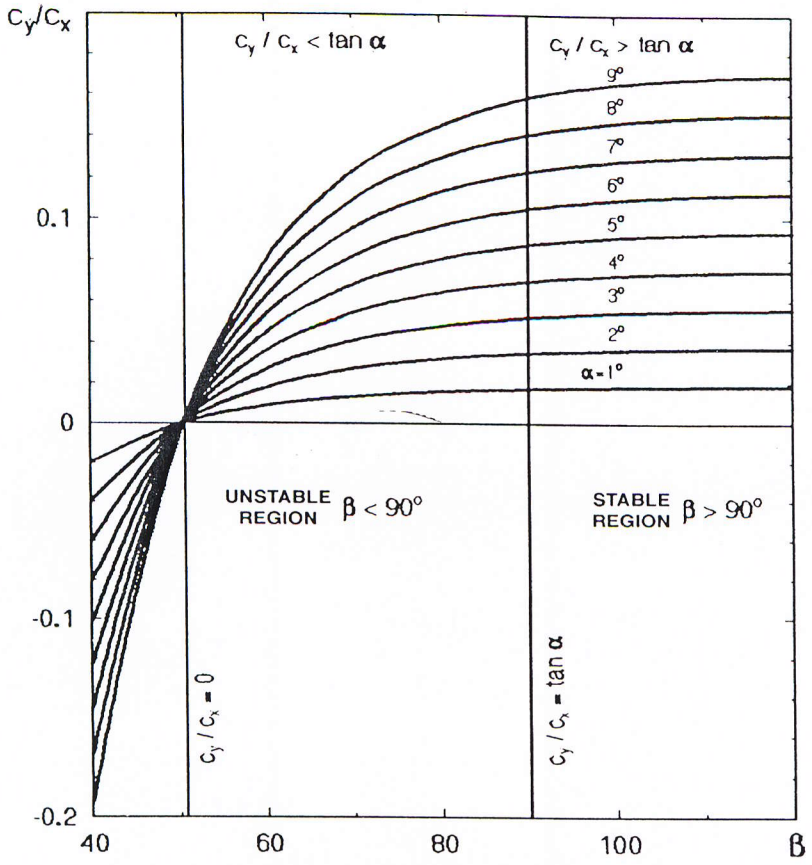

Figure 5. Stability Regions for Cavitating Wedges

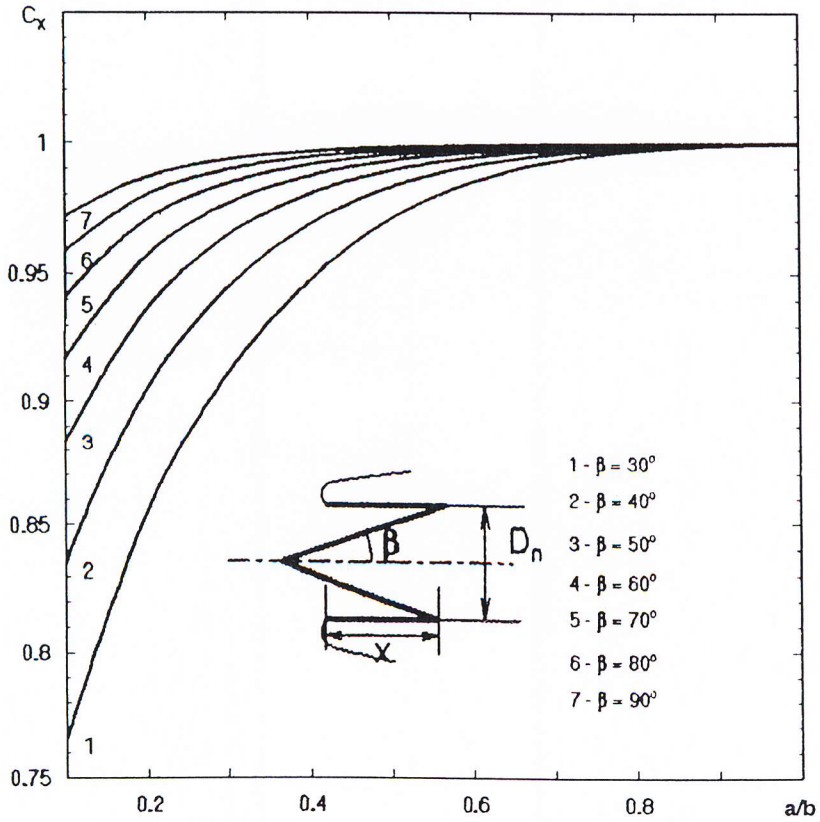

Figure 6. Drag of Σ-Shaped Cavitators

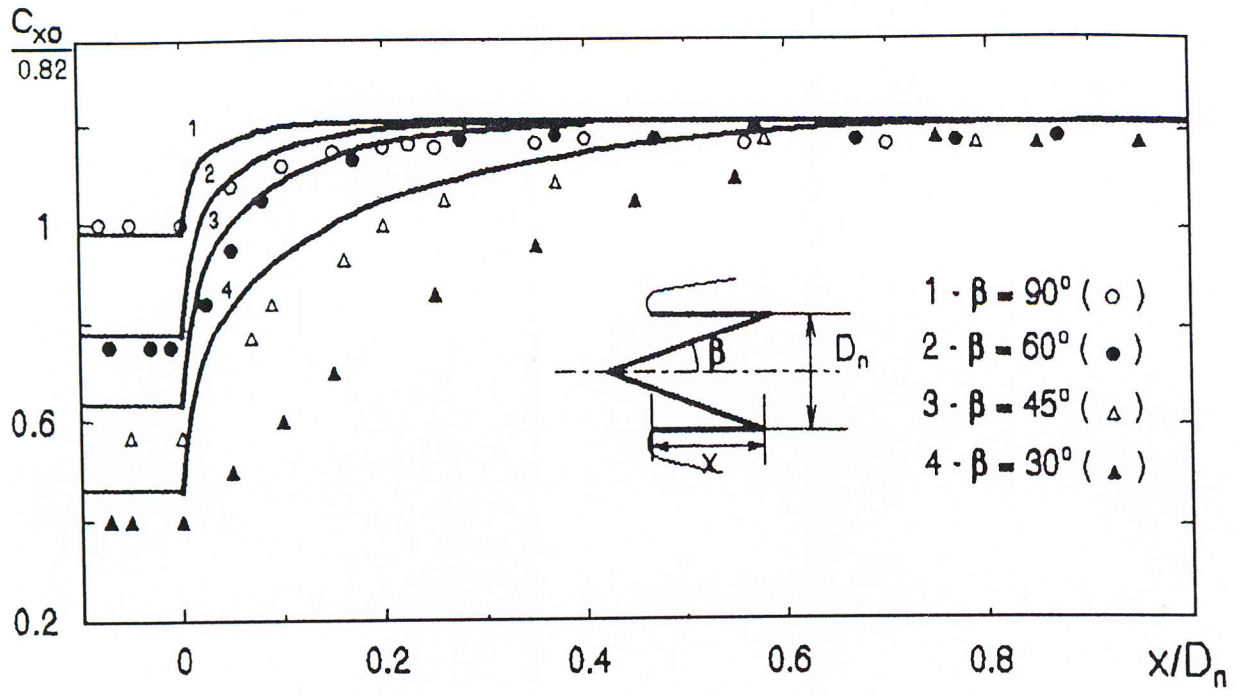

(a)

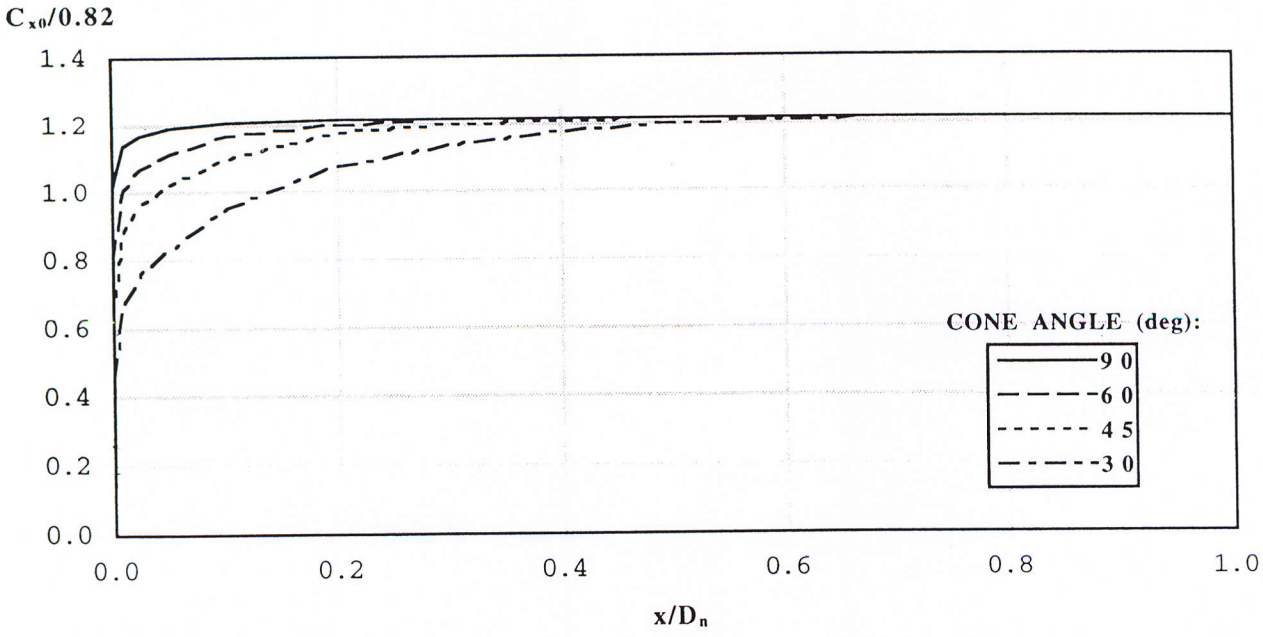

(b)

Figure 7. Drag of Σ-Shaped Cavitators as a Function of Cartridge Extension: (a) Free-Streamline Theory with Circumferential Integration Approximation; (b) Computation Using a Fully-Axisymmetric Boundary-Element Method (Program SCAX)

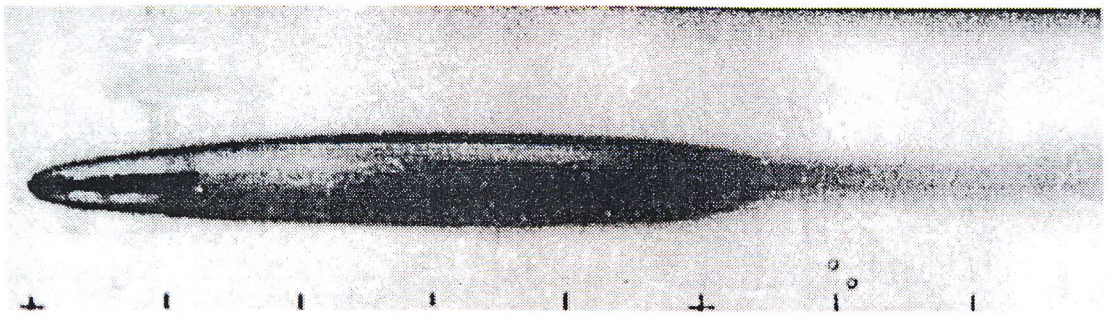

(a)

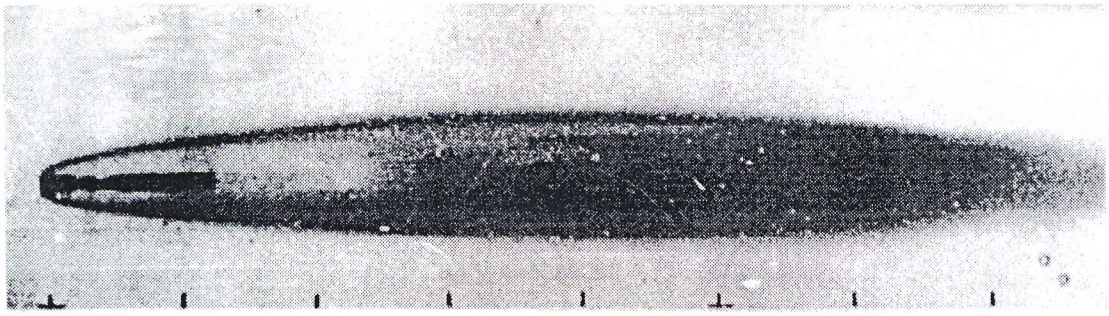

(b)

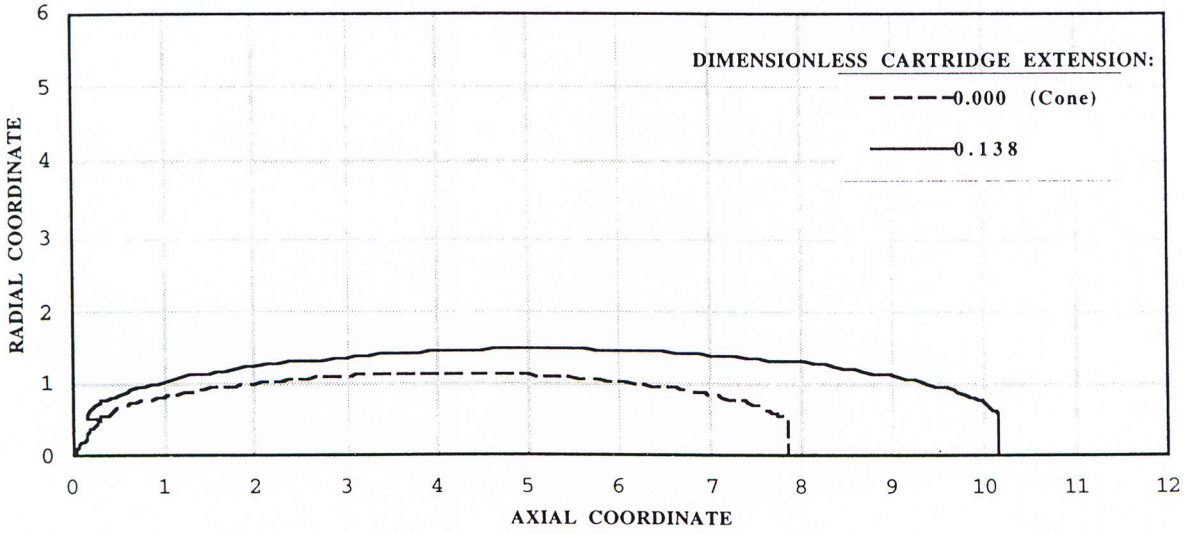

(c)

Figure 8. Supercavities Behind Σ-Shaped Cavitators, μ = 1/3: (a) Experimental Flow Visualization, $x/D_n = 0$, σ = 0.077; (b) Experimental Flow Visualization, $x/D_n = 0.138$ σ = 0.077; (c) Computation Using a Fully-Axisymmetric Boundary-Element Method (Program SCAX), σ = 0.17